Torque Reconstruction for a Full-Scale Maritime Powertrain Using Trend Estimation

Urho Hakonen, Mikael Manngård, Sampo Laine, and Raine Viitala, *Associate Member, IEEE*

***Abstract*—The aim of this article is to present a trend-filtering approach for the simultaneous estimation of unknown input torque and initial states, which can be used to reconstruct the torsional response in the drivetrain of an azimuthing thruster. Accurate information of shaft torques is essential for condition monitoring and improving system design practices. Torque reconstruction with virtual sensors allows more freedom in choosing sensor locations compared to using only physical sensors, and enables the estimation of unknown external disturbances which are difficult to measure directly. Empirical analysis of the torque estimation method is carried out with simulations. Verification is done on experiments on a laboratory testbench and full-scale operational measurements of an azimuthing thruster. The results show that regularized least-squares estimation can be used to accurately estimate propeller shaft torque in a full-scale azimuthing thruster with measurements from the driving motor shaft, by applying regularization constraints based on physical characteristics of the external forces and torsional response of the thruster.**

***Index Terms*—Full-scale azimuthing thruster, input estimation, maritime propulsion, state estimation, torque reconstruction, trend filtering.**

Nomenclature

A	State matrix.
B	Input matrix.
C	Output matrix.
Γ	Impulse response matrix.
d_i	External damping.
I_i	Moment of inertia.
$\mathcal{O}$	Extended observability matrix.
θ_i	Rotational displacement.
τ_i	Internal shaft torque.
v	Noise vector.
x	State vector.
y	Measurement vector.
u	Input vector.
H	Augmented state matrix.
φ	Augmented state vector.
Δ_1	First difference matrix.
Δ_2	Second difference matrix.
$\Delta(\cdot,\cdot)$	First and second difference regularization matrix.
λ	Regularization parameter.
$L(\cdot)$	Regularization function.
I_{N}	N-by-N identity matrix.
k	Discrete-time variable.
k_i	Torsional stiffness.
N	Number of timesteps.
r_i	Gear ratio.
Q	Process noise covariance matrix.
R	Measurement noise covariance matrix.
T_i	External torque.
W_{Q}	Process noise covariance weight matrix.
W_{R}	Measurement noise covariance weight matrix.
u_{m}	Motor input torque.
u_{p}	Propeller input torque.
t	Continuous-time variable.

Received 3 December 2024; revised 19 May 2025; accepted 7 July 2025. Date of publication 24 July 2025; date of current version 19 February 2026. Recommended by Technical Editor J. D. Sanchez Torres and Senior Editor X. Chen. This work was supported in part by the Academy of Finland under Grant 346443, in part by Business Finland (CO-DES Digital transformation of collaborative powertrain design) under Grant 243/31/2022, and in part by Virtual Sea Trial under Grant 7316/31/2023. *(Corresponding author: Urho Hakonen.)*

Urho Hakonen, Sampo Laine, and Raine Viitala are with the Department of Mechanical Engineering, Aalto University, FI-00076 Espoo, Finland (e-mail: urho.hakonen@aalto.fi; sampo.laine@aalto.fi; raine.viitala@aalto.fi).

Mikael Manngård is with the Faculty of Technology and Seafaring, Novia University of Applied Sciences, FI-20100 Turku (Å bo), Finland (e-mail: mikael.manngard@novia.fi).

Color versions of one or more figures in this article are available at https://doi.org/10.1109/TMECH.2025.3587909.

Digital Object Identifier 10.1109/TMECH.2025.3587909

I. Introduction

MARITIME propulsion systems are subject to a large class of torsional excitations during operation. The most concerning excitations originate from hydrodynamic interactions of the propeller and the water body, e.g., during adverse steering conditions and propeller-ice contact. Excitations induce vibrations, which can cause obtrusive noise emissions [1], and potential damage to the powertrain mechanics due to strain and fatigue, which in the worst case lead to total failure of components [2]. Although guidelines regarding propeller excitations for proper design of propulsion systems are described in maritime rules and regulations [3], [4], accurate measurements of the external torques and the torsional response during operation remain important for condition monitoring purposes.

Monitoring torsional vibrations requires measuring the response of the powertrain using, e.g., strain gauges and encoders installed on the propulsion system shafts. Ice-induced propeller loads have been estimated by analyzing the torsional response

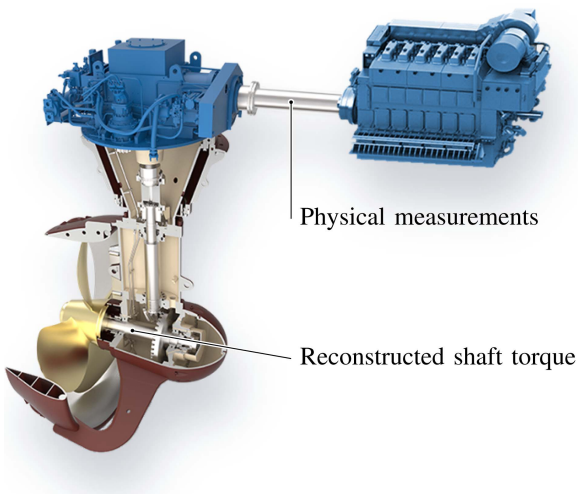

Fig. 1. Example of a Z-drive azimuthing thruster. The thruster consists of a driving motor, shafts, couplings, bevel gears, and a propeller. Shaft torque can be measured with physical sensors near the driving motor and then reconstructed at the propeller shaft with input torque estimates produced using the observer.

measured with strain gauges from the drivetrain of a maritime propulsion system [5], however, such studies are scarce, and the estimates of unknown input torques produced using only physical sensors are limited.

The costs of instrumentation in large maritime propulsion systems can be substantial, thus, only few physical sensors are typically installed on the drivetrain. Furthermore, due to harsh operating conditions, physical measurement equipment is subject to malfunctions, requiring maintenance and sensor replacements. Depending on the location where the equipment is installed, maintenance can be challenging and expensive, especially if dry-docking of the ship is required. To overcome challenges related to physical sensors, methods for reconstructing unknown inputs and states, referred to as observers or "virtual sensors", have been proposed in literature, see, for example, [6] and references therein. Observers provide means for estimating the complete torsional response of a maritime powertrain, using shaft measurements from few locations on the shaft line (Fig. 1). Thus, these kind of observers allow more freedom in choosing sensor locations and the amount of sensors needed for monitoring the torsional response in critical sections of the powertrain.

Estimation of unknown inputs and states can be treated as a filtering problem. Kalman-filtering methods have gained notable interest in simultaneous input and state estimation problems [7], [8], [9], [10], [11]. Kalman filters have been used for torque estimation in applications ranging from different automotive systems [12], [13] to large ship propulsion systems [14], [15]. A challenge with the filtering approach regarding torque estimation is that, as physical input measurements are often not available, it requires an input model based on some assumptions or prior information, e.g., stochastic properties of the unknown inputs [14], [15]. As maritime propulsion systems operate in various conditions, designing an input model for the Kalman filter that accurately describes all types of torsional excitations is challenging. Thus, convex optimization-based methods might provide more flexibility in this regard.

An alternative approach is to consider the reconstruction of unknown input torques as an inverse problem. One option is to use regularized convex optimization methods, which allow straightforward inclusion of problem constraints based on the physical characteristics of the system. In [16], the Kalman filter was reformulated as an ℓ_1-regularized least-squares problem for estimating states and unknown structural disturbances which have step and ramp-like characteristics; however, the problem does not have an analytical solution, requiring an iterative solver. The ℓ_2-regularized least-squares has been successfully applied for torque estimation in maritime propulsion systems [17], [18], [19], [20]. It has an analytical solution, thus, being computationally less demanding than methods requiring iterative solvers. In addition, the ℓ_2-term can be modified to promote smoothness in the estimates. Previously, the estimation of initial state has attained relatively little consideration in torque estimation, even though incorrect information on the initial state can cause notable errors in the reconstructed torque.

This work extends the methodology in [20] by validating its applicability on real-world data and conducting a comprehensive performance analysis. Contributions of this article include batch estimation of both unknown input torques and unknown initial state, which are used to reconstruct the complete torsional response of a Z-drive azimuthing maritime powertrain. The estimation of unknown inputs and initial state is presented as a trend filtering problem, which is based on the ℓ_2-regularized weighted least-squares method. It is shown that the estimation procedure can be improved by applying constraints to the unknown initial state. The proposed method is verified with both laboratory experiments on a small-scale thruster testbench and measurements from a sea trial of a full-scale thruster.

II. Research Methods

The torsional dynamics of an azimuthing thruster were modeled using the shaft-line finite-element method [21], [22] implemented in the open-source library OpenTorsion [23]. The finite element model was formulated as a discrete-time state-space model and extended to be compatible with batch measurements. Estimation of unknown input torques and initial state was presented as a convex trend-filtering optimization problem.

A. Torsional Model of Azimuthing Thruster

The thruster drivetrain is modeled using interconnected lumped elements with inertia I_i, stiffness k_i, and damping c_i (c.f., Fig. 2). Torque losses, e.g., due to viscous friction, can be included in the model as internal damping of the shafts, or external damping d_i. Assuming ideal gears, they can be reduced to single lumped elements by summing the inertias of the pinions $I_i = I_{i,1} + r_i^2 I_{i,2}$, where $r_i = \theta_{i+1}/\theta_i = \dot{\theta}_{i+1}/\dot{\theta}_i$ characterizes the gear ratio.

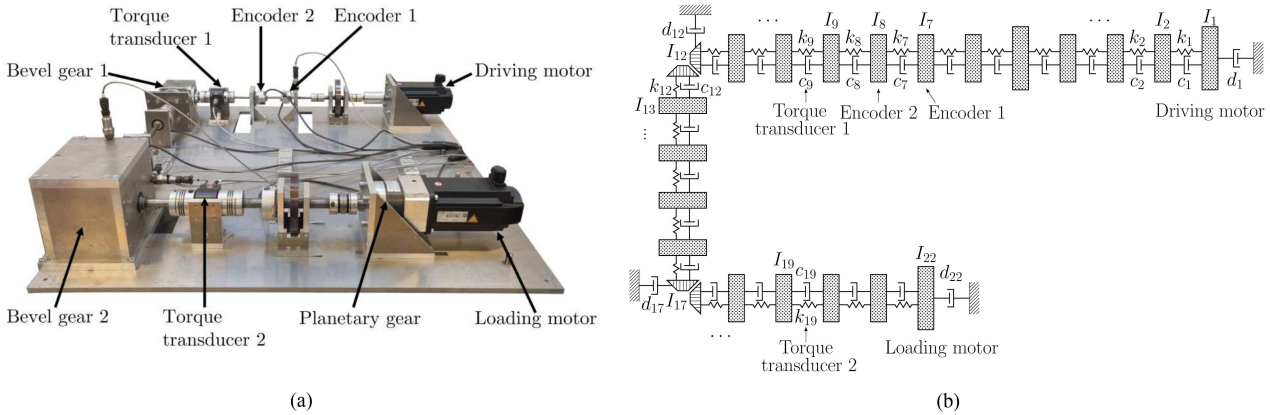

Fig. 2. Small-scale maritime thruster testbench, consisting of shafts, couplings and gears, was driven and loaded using two servomotors. (a) On the driving motor shaft are Encoder 1, Encoder 2 and Torque transducer 1, and on the propeller shaft is Torque transducer 2. (b) A lumped-element model of the testbench. It is assumed that external torque is applied only to the first and last lumped inertias. The model can be utilized to calculate the torsional response, i.e., the internal shaft torque and rotational speed of the lumped-elements. In addition, elements corresponding to the physical sensor locations are annotated in (b).

The equations of motion in terms of the angular displacement θ_i for the ith lumped element, with $i = 1, \ldots, n-1$, are

$$\begin{aligned} I_i\ddot{\theta}_i(t) = {} & c_{i-1}(r_{i-1}\dot{\theta}_{i-1}(t) - \dot{\theta}_i(t)) \\ & - c_i r_i(r_i\dot{\theta}_i(t) - \dot{\theta}_{i+1}(t)) \\ & + k_{i-1}(r_{i-1}\theta_{i-1}(t) - \theta_i(t)) \\ & - k_i r_i(r_i\theta_i(t) - \theta_{i+1}(t)) \\ & - d_i\dot{\theta}_i(t) + T_i(t) \end{aligned} \tag{1}$$

where $T_i(t)$ is external torque applied on the ith lumped element.

The equations of motion (1) of the lumped-element model can be rearranged into a discrete-time linear time-invariant state-space model [14], [15], [21], [23]

$$x(k+1) = Ax(k) + Bu(k), \tag{2}$$

$$y(k) = Cx(k) + v(k) \tag{3}$$

where $x(k) \in \mathbb{R}^n$ is the state vector at k time, with internal torque of shafts $\tau_\mathrm{i} = k_\mathrm{i}(\theta_\mathrm{i} - \theta_{\mathrm{i}+1})$ and angular velocity $\dot{\theta}_\mathrm{i}$ as states. $u(k) \in \mathbb{R}^m$ are unknown torque excitations, $y(k) \in \mathbb{R}^l$ are output measurements, and $v(k) \in \mathbb{R}^l$ measurement noise. The state-space matrices A, B, and C are assembled with the system parameters I_i, c_i, k_i, d_i, and r_i. Explicit structure of the state space matrices is presented in Appendix B. For the present system, it is assumed that input torque

$$u(k) = [u_\mathrm{m}(k) u_\mathrm{p}(k)]^\top$$

is applied only to the first and last lumped elements, corresponding to the driving motor input torque u_m and propeller input torque u_p. The measurement noise is assumed to be a zero-mean stationary-stochastic signal with known covariance

$$\mathrm{E}\left[v(k)v(k)^\top\right] = R. \tag{4}$$

The shaft-line finite element model [Fig. 2(b)] and the state-space model (2)–(3) used in this work were assembled using the OpenTorsion [23] software. The testbench model parameters are presented in Table II in Appendix A. Repeatedly substituting (2) into (3) allows measurements $y(0), y(1), \ldots, y(N-1)$ to be expressed in terms of input torques $u(k)$ and the initial state $x(0)$ in block-matrix form as

$$y = \mathcal{O}x(0) + \Gamma u + v \tag{5}$$

where N is the number of timesteps in the measurement batch, and

$$y = \begin{bmatrix} y(0) \\ y(1) \\ \vdots \\ y(N-1) \end{bmatrix} \quad u = \begin{bmatrix} u(0) \\ u(1) \\ \vdots \\ u(N-1) \end{bmatrix}$$

$$\mathcal{O} = \begin{bmatrix} C \\ CA \\ CA^2 \\ \vdots \\ CA^{N-1} \end{bmatrix} \quad v = \begin{bmatrix} v(0) \\ v(1) \\ \vdots \\ v(N-1) \end{bmatrix}$$

$$\Gamma = \begin{bmatrix} 0 & 0 & 0 & \cdots & 0 \\ CB & 0 & 0 & \cdots & 0 \\ CAB & CB & 0 & & 0 \\ \vdots & & \ddots & \ddots & \\ CA^{N-2}B & CA^{N-3}B & \cdots & CB & 0 \end{bmatrix}.$$

TABLE I
RMSE OF THE SIMULATED TORQUE ESTIMATION EXPERIMENTS

Estimated quantity	RMSE
$\tau(0)$	0.675 N m
$\dot{\theta}(0)$	0.479 rad/s
$u_\mathrm{m}(k)$	0.087 N m
$u_\mathrm{p}(k)$	0.220 N m
$\tau_{20}(k)$	0.247 N m

TABLE II
PARAMETERS OF THE TESTBENCH MECHANICS

Component	Node number n –	Inertia I_n $\mathrm{kg\,m^2}$	Stiffness k_n Nm/rad	Internal Damping c_n Nms/rad	External Damping d_n Nms/rad
Driving motor	1	7.94×10^{-4}	1.90×10^{5}	8.08	0.0030
Shaft	2	3.79×10^{-6}	6.95×10^{3}	0.29	0
Elastomer coupling hub	3	3.00×10^{-6}	90.00	0.24	0
Elastomer coupling middle piece	4	2.00×10^{-6}	90.00	0.24	0
Elastomer coupling hubs and mass	5	7.81×10^{-3}	90.00	0.24	0
Elastomer coupling middle piece	6	2.00×10^{-6}	90.00	0.24	0
Elastomer coupling hub and shaft	7	3.29×10^{-6}	94.06	0	0
Shaft, encoder and coupling	8	5.01×10^{-5}	4.19×10^{4}	1.78	0
Torque transducer	9	6.50×10^{-6}	5.40×10^{3}	0.23	0
Coupling	10	5.65×10^{-5}	4.19×10^{4}	1.78	0
Shaft	11	4.27×10^{-6}	1.22×10^{3}	0.52	0
Bevel gear and shaft	12	3.25×10^{-4}	4.33×10^{4}	1.84	0.0042
Coupling	13	1.20×10^{-4}	3.10×10^{4}	1.32	0
Shaft	14	1.15×10^{-5}	1.14×10^{3}	0.05	0
Shaft and coupling	15	1.32×10^{-4}	3.10×10^{4}	1.32	0
Shaft	16	4.27×10^{-6}	1.22×10^{4}	0.52	0
Bevel gear and shaft	17	2.69×10^{-4}	4.43×10^{4}	1.88	0.0042
Coupling	18	1.80×10^{-4}	1.38×10^{5}	5.86	0
Torque transducer	19	2.00×10^{-5}	2.00×10^{4}	0.85	0
Coupling	20	2.00×10^{-4}	1.38×10^{5}	5.86	0
Shaft	21	4.27×10^{-6}	1.22×10^{4}	0.52	0
Mass and loading motor	22	4.95×10^{-2}	–	–	0.24

Assessing the observability and controllability of the system provide important insight on the identifiability of unknown states and inputs. The n states of the system are observable if $\mathrm{rank}[\mathcal{O}(A,C)]=n$, and the system is controllable if $\mathrm{rank}[\mathcal{O}(A^\top,B^\top)]=n$. The torsional vibration model does not fulfill these criteria, thus, the torque estimation problem is ill-posed, however, regularization methods can be used to improve the conditioning of the problem.

B. Convex Optimization Problem

The input reconstruction problem can be formulated as a regularized weighted least-squares problem

$$\begin{aligned}\underset{u,v}{\text{minimize}}\quad & \frac{1}{N}\sum_{k=0}^{N-1} v(k)^\top R^{-1} v(k) + L(u)\\ \text{subject to}\quad & v = y - \mathcal{O}x(0) - \Gamma u\end{aligned} \tag{6}$$

for a known initial state $x(0)$. The regularization term $L(u)$ is used to ensure the least-squares problem is well posed. The regularization function $L(u)$ should be determined based on known properties of the unknown input signal u.

For stationary-stochastic zero-mean input excitations with known covariance, $\mathrm{E}[u(k)u^\top(k)]=Q$, the regularization term can be set to

$$L(u) = \frac{1}{N}\sum_{k=0}^{N-1} u^\top(k) Q^{-1} u(k) \tag{7}$$

which results in the weighted Tikhonov-regularized problem

$$\begin{aligned}\underset{u,v}{\text{minimize}}\quad & \frac{1}{N}\sum_{k=0}^{N-1} \left(v(k)^\top R^{-1} v(k) + u(k)^\top Q^{-1} u(k)\right)\\ \text{subject to}\quad & v = y - \mathcal{O}x(0) - \Gamma u.\end{aligned} \tag{8}$$

By defining the matrices $W_\mathrm{R} = I_N \otimes R^{-1}$ and $W_\mathrm{Q} = I_N \otimes Q^{-1}$, the problem has an analytical solution

$$\hat{u} = \left(W_\mathrm{Q} + \Gamma^\top W_\mathrm{R}\Gamma\right)^{-1}\Gamma^\top W_\mathrm{R}\left(y - \mathcal{O}x(0)\right). \tag{9}$$

Finally, the complete torsional response of the system can be reconstructed with $x(0)$ and $\hat{u}$ using (5)

$$\hat{y} = \mathcal{O}x(0) + \Gamma\hat{u} \tag{10}$$

where $\hat{y}$ is the estimated torsional response. It should be noted that accurate knowledge of $x(0)$ is rarely available, and maritime propulsion systems can be affected by input torques u which are not zero-mean and stationary-stochastic.

C. Trend Filter Formulation

In addition to the unknown input torque, knowledge of the initial state is required to accurately reconstruct the torsional response of a maritime propulsion system. The estimation of unknown input torques $u(k)$ and initial state $x(0)$ can be formulated as a regularized weighted least-squares problem

$$\begin{aligned}\underset{\varphi,v}{\text{minimize}}\quad & v^\top W_\mathrm{R} v + L(\varphi)\\ \text{subject to}\quad & v = y - H\varphi\end{aligned} \tag{11}$$

where $H=[\mathcal{O}\Gamma]$, $\varphi=[x(0)^\top u(k)^\top]^\top$.

The regularization function $L(\varphi)$ is used to improve the conditioning of the weighted least-squares problem by enforcing desired constraints on the unknown input torques u and initial state $x(0)$. The constraints should be based on known properties of both u and $x(0)$.

The optimization problem can be formulated to promote smoothness in input estimates by constraining the second difference of u with

$$\sum_{k=1}^{N-2}(u(k-1)-2u(k)+u(k+1))^2 = \|\Delta_2 u\|_2^2. \tag{12}$$

That is to say, for input torques u_m and u_p, the regularization term is

$$\Delta_2 u = \begin{bmatrix} 1 & 0 & -2 & 0 & 1 & & \\ & 1 & 0 & -2 & 0 & 1 & \\ & & \ddots & \ddots & \ddots & \ddots & \\ & & 1 & 0 & -2 & 0 & 1 \\ & & & 1 & 0 & -2 & 0 & 1 \end{bmatrix} \begin{bmatrix} u_\mathrm{m}(0) \\ u_\mathrm{p}(0) \\ \vdots \\ u_\mathrm{m}(k) \\ u_\mathrm{p}(k) \end{bmatrix}. \tag{13}$$

This approach bears resemblance to Hodrick–Prescott trend filtering [24], where the goal is to find a tradeoff between the smoothness of estimates and the residual error, however, here the second order dynamics of the system are properly accounted for.

Regarding the initial conditions, it seems reasonable to assume that the states of coupled elements, i.e., the rotating speed of two adjacent lumped masses, are relatively close to each other. Thus, a feasible set of solutions for the unknown initial state can be ensured by defining a regularization term for $x(0)$ in a similar fashion as for the input, by constraining the first difference of the initial state variables. Based on the assumption, regularization term for the initial state is defined as

$$\Delta_1 x(0) = \begin{bmatrix} 1 & -1 & & & & & & \\ & 1 & -1 & & & & & \\ & & \ddots & \ddots & & & & \\ & & & 1 & -1 & & & \\ & & & & 1 & -1 & & \\ & & & & & \ddots & \ddots & \end{bmatrix} \begin{bmatrix} \tau_1(0) \\ \tau_2(0) \\ \vdots \\ \dot{\theta}_1(0) \\ \dot{\theta}_2(0) \\ \vdots \end{bmatrix}. \tag{14}$$

It should be noted that there are zero rows in Δ_1 where the aforementioned assumption does not hold, i.e., at gear locations, and where the physical state quantities are different to ensure for these rows, that rotational speed is not subtracted from torque.

The complete regularization function used in (11) can now be formulated as

$$L(\varphi) = \left\| \underbrace{\begin{bmatrix} \lambda_1\Delta_1 & 0 \\ 0 & \lambda_2\Delta_2 \end{bmatrix}}_{\Delta(\lambda_1,\lambda_2)} \underbrace{\begin{bmatrix} x(0) \\ u \end{bmatrix}}_{\varphi} \right\|_2^2 \tag{15}$$

where the matrix $\Delta(\lambda_1,\lambda_2)$ consists of the first and second difference matrices, and λ_1 and λ_2 are user defined parameters which scale how strictly regularization is enforced.

For practical applications, the regularization parameter λ is often determined using heuristic methods, e.g., the L-curve [25],

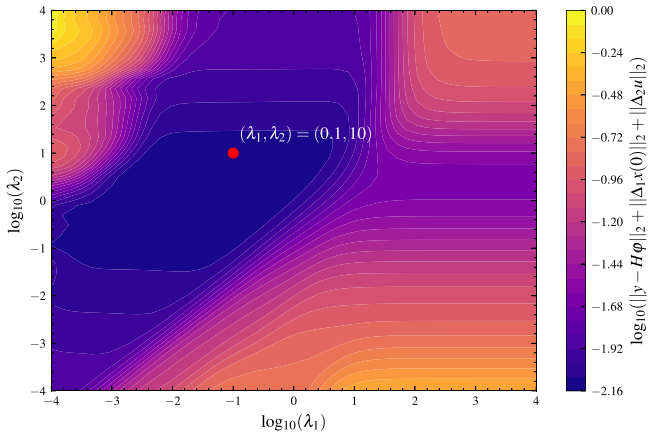

Fig. 3. Normalized sum of the residual norm and solution norm when the regularization parameter values are varied $\lambda_1=\lambda_2=10^{-4},\ldots,10^4$ in logarithmic scale. The red dot highlights a point $(\lambda_1,\lambda_2)=(0.1,10)$, in the region where the sum of the norms is small.

where a pareto-optimal λ can be found by comparing the norm sizes of the regularization term $L(u)$ and the residual v. However, the L-curve is not sufficient for determining two regularization parameters simultaneously. Instead, a heuristic approach inspired by the principles of L-curve is used for finding suitable values (λ_1,λ_2). The regularization parameters are searched by performing torque estimation using simulated measurements for a range of values λ_1 and λ_2. The simulated measurements are described later in Section II-D. The sum of the residual norm and norm of the regularization term for each point (λ_1,λ_2) is shown in Fig. 3. A pareto-efficient (λ_1,λ_2) is found where the sum of the norms is small. The proposed torque estimation method does not appear to be particularly sensitive to λ_1 or λ_2, thus, it is assumed that more than one pair (λ_1,λ_2) could be used to produce accurate torque estimates. Simultaneously, there remains a possibility to adjust how strongly regularization is applied to the unknown initial state and input torques without compromising estimation accuracy. Comparison of estimates for different (λ_1,λ_2) is considered later in Section III.

Finally, with (11) and (15) the ℓ_2-regularized weighted least-squares problem can be written as

$$\begin{aligned} \underset{\varphi,v}{\text{minimize}} \quad & v^\top W_\mathrm{R} v + \|\Delta(\lambda_1,\lambda_2)\varphi\|_2^2 \\ \text{subject to} \quad & v = y - H\varphi \end{aligned} \tag{16}$$

which has an analytical solution

$$\hat{\varphi} = \left(\Delta(\lambda_1,\lambda_2)^\top\Delta(\lambda_1,\lambda_2) + H^\top W_\mathrm{R} H\right)^{-1} H^\top W_\mathrm{R} y \tag{17}$$

where $\hat{\varphi}$ is an estimate of the augmented state vector containing the initial state and input torques. The KKT conditions for the optimality of the analytical solution are presented in Appendix C. Subsequently, the torsional response can be reconstructed with

$$\hat{y} = H\hat{\varphi} \tag{18}$$

where $\hat{y}$ contains shaft torque and rotational speed estimates.

D. Experimental Verification

Verification of torque estimation by trend filtering was performed using a small-scale maritime thruster testbench shown in Fig. 2. The testbench consists of shafts, couplings, two bevel gears, and a planetary gear. The gear ratios are 3:1, 4:1, and 1:8, respectively. Two 2.63-kW Bosch Rexroth MS2N06 synchronous servomotors installed on the ends of the drivetrain were used for driving and applying loads on the testbench. The testbench is designed to have its lowest torsional natural frequencies and the angular displacement of the shafts under nominal load comparable to a full-scale system. The testbench was equipped with two Heidenhain incremental encoders and one strain gauge-based ETH-Messtechnic torque transducer on the driving motor shaft and another on the propeller shaft. For a more detailed description of the testbench the reader is referred to [26].

The small-scale maritime thruster testbench was modeled using the shaft-line FEM as described in Section II-A. Parameters of the testbench model are presented in Table II. Simulations with the testbench model were used for theoretical analysis of the torque estimation method presented in Section II-C. Simulation time was 1.5 s with step size $\Delta t = 0.001$ s. A constant torque $u_\mathrm{m} = 2.8$ Nm was applied on the lumped element corresponding to the driving motor, while at $t = 0.7$ s an impulse, consisting of equally long upward and downward ramp of in total 56 time steps with a maximum value of $u_\mathrm{p} = 10$ Nm, was applied to the element corresponding to the loading motor. Similar to the physical sensors installed on the testbench (Fig. 2), simulated rotational speed and shaft torque measurements were used in the estimation of input torques and initial state, and subsequent reconstruction of the torsional response of the testbench. Explicit structure of the measurement vector for the testbench model was

$$y(k) = \left[\tau_8(k) \dot{\theta}_5(k) \dot{\theta}_6(k)\right]^\top$$

where the indexing refers to the lumped element nodes. Gaussian white noise with standard deviation $\sigma = 0.1$ was added to include measurement error in the simulation. The simulated measurements were divided in to batches of 500 timesteps. Values of regularization parameters of the trend filter (17) were $\lambda_1 = 0.1$ and $\lambda_2 = 10$ (c.f., Fig. 3). Fig. 4 presents the results of the simulated torque estimation experiment. Estimates of the unknown input torques and initial state allow reconstructing the torsional response accurately.

Performance of the trend filter method in the simulated impulse experiment was analyzed using the Monte Carlo method. Gaussian white noise with $\sigma = 0.1$ was included in 2000 instances of simulated measurements, which were subsequently used to perform torque estimation. The total root mean square error (RMSE) over the 2000 simulations was calculated for the initial state $\tau(0)$ and $\dot{\theta}(0)$, the input torques $u_\mathrm{m}(k)$ and $u_\mathrm{p}(k)$, and the internal propeller shaft torque $\tau_{20}(k)$. The resulting RMSE values are presented in Table I.

III. Results

Verification of the proposed trend-filtering method for estimation of unknown input torques and torsional response

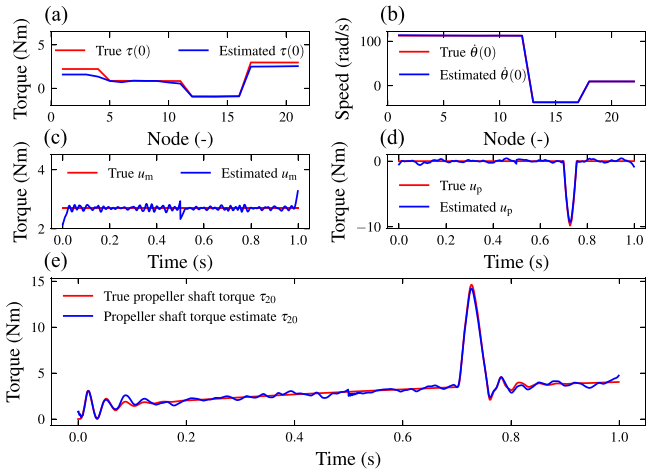

Fig. 4. Simulation experiment of torque estimation using the testbench model. Estimated initial state at the beginning of the second batch, including (a) shaft torques $\tau(0)$ and (b) rotational speeds $\dot{\theta}(0)$ in terms of lumped-element node values, estimated input torques of (c) driving motor u_m and (d) loading motor u_p, and (e) the reconstructed propeller shaft torque τ_{20} compared to true values.

for an azimuthing thruster was conducted in two parts. First, an ice excitation experiment was conducted on the laboratory-scale testbench presented in Section II-D. Then, estimation of propeller shaft torque in a full-scale azimuthing thruster was performed using operational measurements from a sea trial. The experiments were conducted offline, i.e., measurement data was first collected, and then torque estimation was performed.

A. Torque Estimation for Small-Scale Thruster Testbench

An ice excitation experiment was conducted on the laboratory-scale testbench. The ice excitation profile was modeled according to the description in maritime regulations [3], [4]. The excitation consisted of consecutive impulses with a half-sinusoidal shape, emulating propeller blades striking blocks of ice. The driving motor speed was kept constant at 2000 r/min while the loading motor was used to apply the ice excitation to the testbench drivetrain. Shaft torque and speed were measured close to the driving motor [c.f., Fig. 2(a)] to be used in torque estimation. Shaft torque close to the loading motor was measured for verification of the estimation results.

For the ice excitation experiment, the model structure was the same as in the simulated experiment in Section II-D. The measurements were divided to batches of 500 time steps. The measurement error covariance matrix used was $R = \mathrm{diag}([0.05 0.10 .20])$, which was determined using measurements from the testbench. The regularization parameter values used were $\lambda_1 = 0.1$ and $\lambda_2 = 10$. The regularization parameters were determined based on the simulation results described in Section II-C.

Fig. 5(a) and (b) present the estimated input torques from the driving and loading motors, and (c) the reconstructed propeller shaft torque compared to reference measurements. The trend filter produced a smooth estimate which closely matches the physical measurement. A small transient, e.g., at $t = 4.48$ s in

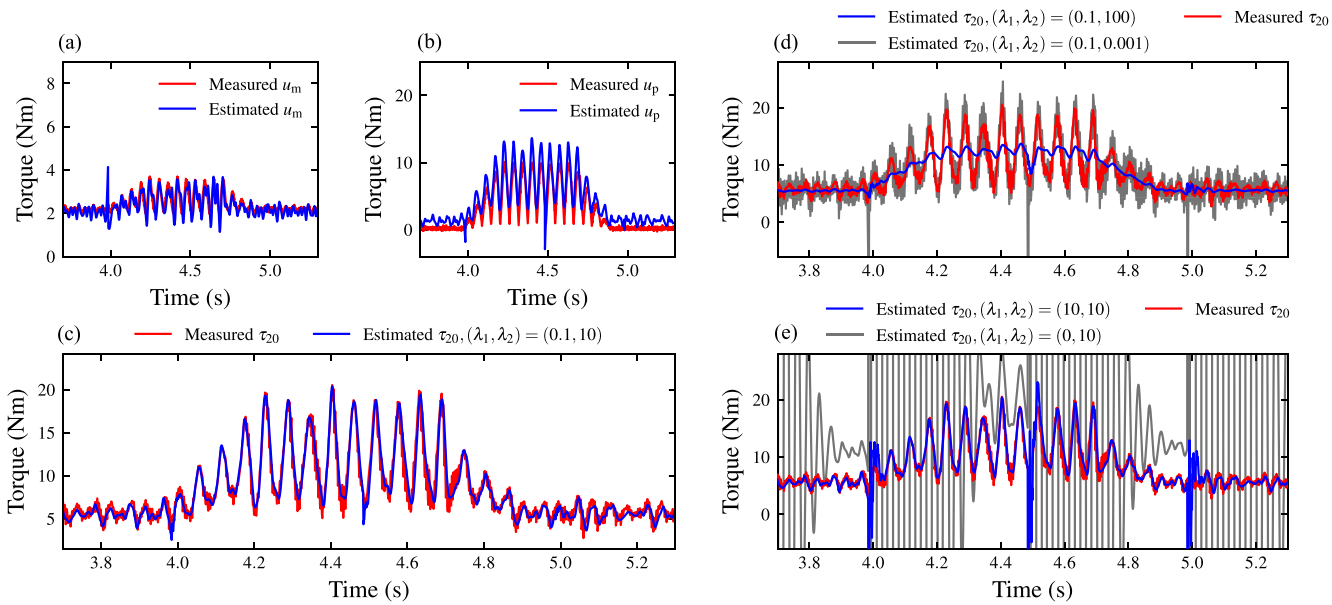

Fig. 5. (a) Driving motor torque, (b) loading motor torque, and (c) propeller shaft torque estimates with $(\lambda_1, \lambda_2) = (0.1, 10)$ compared to measurements on the testbench in an ice excitation experiment. The driving motor speed was kept constant at 2000 r/min while a series of torque impulses, shown in (b), were applied on the drivetrain using the loading motor. Shaft torque estimates with different values λ are shown in (d) and (e). In (d), the blue line is the estimate with $(\lambda_1, \lambda_2) = (0.1, 100)$, and the gray line with $(\lambda_1, \lambda_2) = (0.1, 0.001)$. In (e), the blue line is the estimate with $(\lambda_1, \lambda_2) = (10, 10)$, and the gray line with $(\lambda_1, \lambda_2) = (0, 10)$.

Fig. 5, which is most likely not part of the motor input torques, can be seen in the input estimates. It occurs at the beginning of measurement batches used in the estimation. It is related to the least-squares solution, however, its effect on the reconstructed propeller shaft torque is small. Fig. 5(d) and (e) show the torque estimation experiment with different values (λ_1, λ_2). Increasing λ_2 makes the torque estimate smoother and vice versa. Both too large and too small values λ_1 can result in poor initial state estimates, which can be seen as large impulses in the reconstructed torsional response. When regularization was not applied to the unknown initial state, i.e., $\lambda_1 = 0$, the reconstructed shaft torque included impulses orders of magnitude larger than the measured shaft torque. The impulses are a result of poor initial state estimates, which can be explained by the ill-posedness of the unregularized least-squares problem.

B. Torque Estimation for a Full-Scale Thruster

Torque and speed from the shafts of a full-scale azimuthing thruster were measured during a sea trial. A section of the dataset, during which the propulsion system was driven at a constant speed, was used for estimating propeller shaft torque. As is often the case in full-scale operational measurements, the motor shaft speed data contained some notable measurement errors caused by sensor issues. Furthermore, the propeller shaft torque data contained a frequency component matching the propeller shaft rotational speed, which was not visible in the motor shaft torque data. This could be due to alignment error in installation of the strain gauges, causing the bending of the propeller shaft to be visible in the measurements. The measurement errors were included in the data used in torque estimation. Parameters of the full-scale thruster model are given in Table III. The gear ratios of the upper and lower bevel gears are 17:42 and 14:38, respectively. The parameters were provided by the OEM.

Results of the full-scale torque estimation are presented in Fig. 6. The used regularization parameters were $\lambda_1 = 0.0001$ and $\lambda_2 = 1$. The regularization parameters were chosen similarly to those used in the testbench experiments. Comparing the frequency spectra of the measured and estimated propeller shaft torque showed that the components corresponding to the first torsional natural frequency, propeller blade frequency and motor shaft rotational frequency could be estimated. The differences in amplitude could be explained by inaccurate modeling of viscous damping in the drivetrain, or other inaccuracies in the full-scale thruster parameters provided by the OEM. Physical measurements of the external torques were not available.

IV. Discussion

The proposed trend filtering method contributes to the improving condition monitoring procedures of maritime propulsion systems. The system dynamics have to be properly taken into account when estimating torque, especially during large torque variations. Accurate information on the large shaft torque variations in the propulsion system allows proper maintenance scheduling and avoiding fatal scenarios such as failure of mechanical components. With industry-standard modeling methods, application of the torque estimation procedure is straightforward for various different systems.

Compared to conventional Kalman-filter methods, the trend-filter formulation simplifies the imposition of additional constraints such as ensuring smoothness in the estimates. This

TABLE III
PARAMETERS OF THE FULL-SCALE THRUSTER MECHANICS

Component	**Node number** n –	**Inertia** I_n $\mathrm{kg\,m^2}$	**Stiffness** k_n $\mathrm{Nm/rad}$	**Internal Damping** c_n $\mathrm{Nms/rad}$	**External Damping** d_n $\mathrm{Nms/rad}$
Engine part 1	1	1.94	39.00×10^3	226	0
Engine part 2	2	2.37	12.00×10^6	10.79×10^3	0
Engine part 3	3	2.02	8.66×10^6	7.78×10^3	4.62
Engine part 4	4	1.94	8.66×10^6	7.78×10^3	4.62
Engine part 5	5	1.96	8.47×10^6	7.61×10^3	4.62
Engine part 6	6	1.96	8.66×10^6	7.78×10^3	4.62
Engine part 7	7	1.94	8.66×10^6	7.78×10^3	4.62
Engine part 8	8	2.02	12.00×10^6	10.79×10^3	4.62
Flexible coupling part 1	9	25.79	66.00×10^3	0.18	7.69
Flexible coupling part 2	10	2.31	1.60×10^6	0.20×10^3	0
Motor shaft part 1	11	2.36	60.00×10^6	7.55×10^3	0
Motor shaft part 2	12	3.57	10.29×10^6	1.29×10^3	0.0042
Motor shaft part 3	13	2.79	9.18×10^6	1.16×10^3	0
Upper bevel gear and coupling	14	2.00	8.25×10^6	1.04×10^3	7.4
Vertical shaft part 1	15	1.54	57.76×10^6	7.27×10^3	0
Vertical shaft part 2	16	2.18	4.66×10^6	0.59×10^3	0
Lower bevel gear and propeller shaft	17	5.36	25.40×10^6	3.20×10^3	7.4
Propeller	18	716.60	–	–	0

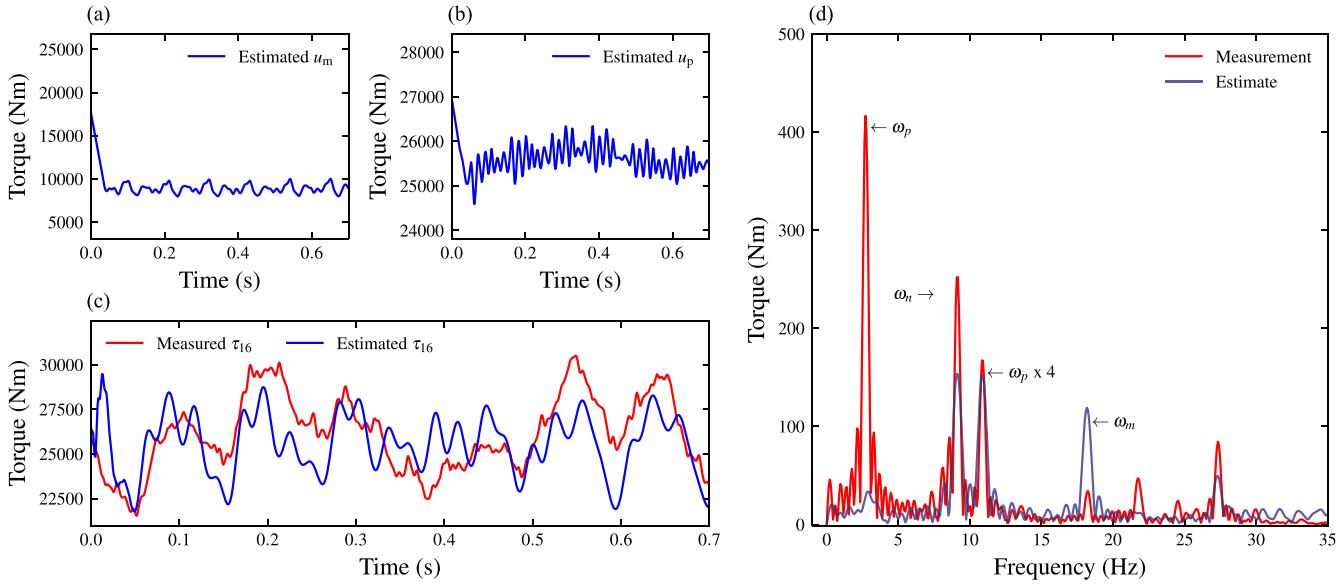

Fig. 6. Torque estimates produced with the trend filter compared to measurements from the propeller shaft of the full-scale azimuthing thruster, (a) estimated driving motor input torque, (b) estimated propeller input torque, (c) estimated propeller shaft torque, and (d) frequency spectra of the measured and estimated propeller shaft torques, where the propeller rotational frequency ω_p, the first torsional natural frequency ω_n, the first blade frequency $4 \times \omega_\mathrm{p}$, and the motor shaft rotational frequency ω_m are annotated in the figure, respectively.

makes the design of torque observers more convenient and flexible. Constraints in torque estimation aid in ensuring that the reconstructed signals adhere to physical principles. Furthermore, real-time torque estimation remains possible, as the analytical solution of the trend filtering problem (17) can be partially precomputed, i.e., only the measurement vector y changes across data batches, provided that the regularization parameters are defined prior to estimation. In this study, the regularization parameters λ_1 and λ_2 were determined using simulations with a torsional vibration model. This does not guarantee that the regularization parameters are necessarily as pareto-efficient as possible for all data batches used in torque estimation, but it is computationally less demanding compared to searching the λ_1, λ_2 for each individual data batch separately.

Results of the simulated experiments showed that the proposed approach can be used to produce smooth and accurate estimates of the unknown input torques and torsional response, which was further verified with physical measurements on the laboratory testbench. By constraining the unknown initial state, the torsional response could be reconstructed without the need to rely on only the impulse response of the torsional vibration model or prior knowledge of the true initial state. The transition between measurement batches was carried out by overlapping

the last and first timesteps of consecutive batches. A larger overlap would make the transition between batches smoother [20]. Alternatively, methods utilizing a sliding time-window could be used. However, these approaches come with increased computational cost.

Regarding the full-scale experiment, taking into account the sensor issues and possible inaccuracies in the thruster parameters, the trend filter performed well, producing smooth estimates of the propeller shaft torque. The full-scale measurements used in this research did not include transient phenomena, such as propeller-ice contact, and these kind of measurements are generally rare. The proposed torque estimation method should be further verified with full-scale measurements, which include, e.g., ice excitations. Furthermore, other methods than ℓ_2-regularization could be explored for the purpose of torque estimation in maritime propulsion systems.

V. Conclusion

This article presented the estimation of unknown input torque and initial state using trend filtering, with subsequent reconstruction of the full torsional response of a maritime propulsion system. Torque estimation was performed for both a laboratory-scale thruster testbench and a full-scale Z-drive thruster, using measurements from a shaft close to the driving motor. By applying regularization to the unknown initial state and input torques, the trend filter produced smooth and accurate estimates of the propeller shaft torque.

Appendix A
Parameters of the Laboratory-Scale Testbench and Full-Scale Thruster Models

Parameters of the drivetrain mechanics of the small-scale thruster testbench are presented in Table II. Parameters of the drivetrain mechanics of the full-scale thruster are presented in Table III.

Appendix B
State-Space Matrices for Torsional Vibration Model of a Thruster

The equations of motion (1) of the torsional vibration model are assembled to matrix form

$$M\ddot{\theta}(t) + D\dot{\theta}(t) + K\theta(t) \tag{B1}$$

where the vector $\theta(t)$ contains rotational angles, the mass matrix M contains inertia values I_i, the damping matrix D contains damping values c_i and d_i, and the stiffness matrix K contains torsional stiffness values k_i. For a detailed description of the assembly of the system matrices, including the modeling of the gears as single lumped inertias with a gear ratio r_i, the reader is referred to [21] and [23].

The state-space form of (B1) can be formulated as

$$A_s = \begin{bmatrix} 0 & I \\ -M^{-1}K & -M^{-1}K \end{bmatrix} \quad B_s = \begin{bmatrix} 0 \\ M^{-1} \end{bmatrix} \tag{B2}$$

where A_s and B_s are conventional state-space matrices for a torsional vibration model with the state vector $x(t)$ consisting of rotational displacements and rotational speeds $x(t) = [\theta_i(t), \ldots, \dot{\theta}_i(t), \ldots]^\top$. Instead of θ_i, the state space model can be modified to include internal shaft torques in the state vector $x(t) = [\tau_i(t), \ldots, \dot{\theta}_i(t), \ldots]^\top$, by utilizing the relation $\tau_i = k_i(r_i\theta_i - \theta_{i+1})$ in matrix form, i.e.,

$$X = \begin{bmatrix} r_1k_1 & -k_1 & 0 & & & & & \\ 0 & \ddots & \ddots & \ddots & & & & \\ & \ddots & r_{n-1}k_n & -k_n & \ddots & & & \\ & & \ddots & 0 & 1 & \ddots & & \\ & & & \ddots & \ddots & \ddots & 0 & \\ & & & & 0 & 0 & 1 & \end{bmatrix}. \tag{B3}$$

The transformation is carried out as follows:

$$\begin{aligned} A &= XA_sX^{-1} \\ B &= XB_s \end{aligned} \tag{B4}$$

resulting in the state-space system (2), which is compatible with a state vector consisting of shaft torque and rotational speed values. The output matrix C connects the states x to the measurements y, and its structure is application specific. For the testbench model used in the experiments in Section II-D

$$C = \begin{bmatrix} 0 & \cdots & 1_{\tau_8} & \cdots & & 0 \\ 0 & & \cdots & 1_{\theta_5} & \cdots & 0 \\ 0 & & & \cdots & 1_{\theta_6} & \cdots & 0 \end{bmatrix} \tag{B5}$$

where the indexing refers to the measured quantity in the state vector.

Appendix C
Karush–Kuhn–Tucker Conditions for the ℓ_2-Regularized Least-Squares Problem

The convex optimization problem (16) can be written as

$$\begin{aligned} \underset{\varphi, v}{\text{minimize}} \quad & v^\top W_\mathrm{R} v + (\Delta\varphi)^\top(\Delta\varphi) \\ \text{subject to} \quad & v = y - H\varphi \end{aligned} \tag{C1}$$

where $\Delta = \Delta(\lambda_1, \lambda_2)$. By forming the Lagrangian function

$$\mathcal{L}(\varphi, v, \nu) = v^\top W_\mathrm{R} v + (\Delta\varphi)^\top(\Delta\varphi) + \nu(y - H\varphi - v) \tag{C2}$$

where $\nu \in \mathbb{R}^l$ is a Lagrange multiplier, the stationarity conditions can be derived as

$$\begin{aligned} \partial_\varphi \mathcal{L}(\varphi, v, \nu) &= 2\Delta^\top\Delta\varphi - H^\top\nu = 0 \\ \partial_v \mathcal{L}(\varphi, v, \nu) &= 2W_\mathrm{R} v - \nu = 0 \end{aligned} \tag{C3}$$

and the primal feasibility condition is

$$v = y - H\varphi. \tag{C4}$$

The stationarity conditions (C3) yield the normal equation

$$\left(H^\top W_\mathrm{R} H + \Delta^\top\Delta\right)\varphi = H^\top W_\mathrm{R} y \tag{C5}$$

which gives the analytical solution (17) for the weighted ℓ_2-regularized least-squares problem.

ACKNOWLEDGMENT

The authors would like to thank Kongsberg Maritime Finland Oy for their work and support regarding the small-scale maritime thruster testbench, and for providing the full-scale thruster model parameters and measurements.

REFERENCES

[1] J. Willie and R. Sachs, "Structural and torsional vibration and noise analysis of a dry screw compressor," *Proc. Inst. Mech. Engineers, Part E: J. Process Mech. Eng.*, vol. 231, no. 1, pp. 4–13, 2017.
[2] G. Vizentin, G. Vukelic, L. Murawski, N. Recho, and J. Orovic, "Marine propulsion system failures—A review," *J. Mar. Sci. Eng.*, vol. 8, no. 9, pp. 1–14, 2020.
[3] DNV, "Ships for navigation in ice," *Det Norsk Veritas (DNV)*, Regulation, 2011.
[4] TRAFI, "Ice class regulations and the application thereof," *Finnish Transport Saf. Agency (Trafi)*, Regulation, 2021.
[5] M. Suominen et al., "Full-scale measurements on-board psrv s.a. agulhas ii in the baltic sea," in *Proc. 22nd Int. Conf. Port Ocean Eng. under Arctic Conditions*, 2013.
[6] S. Khan, K. A. Pant, and I. Hwang, "Synthesis of robust state estimation algorithms under unknown sensor inputs," *IEEE Control Syst. Lett.*, vol. 7, pp. 2707–2712, 2023.
[7] S. Gillijns and B. De Moor, "Unbiased minimum-variance input and state estimation for linear discrete-time systems," *Automatica*, vol. 43, no. 1, pp. 111–116, 2007.
[8] E. Lourens, E. Reynders, G. De Roeck, G. Degrande, and G. Lombaert, "An augmented Kalman filter for force identification in structural dynamics," *Mech. Syst. Signal Process.*, vol. 27, pp. 446–460, 2012.
[9] R. R. Bitmead, M. Hovd, and M. A. Abooshahab, "A Kalman-filtering derivation of simultaneous input and state estimation," *Automatica*, vol. 108, 2019, Art. no. 108478.
[10] U. Lagerblad, H. Wentzel, and A. Kulachenko, "Study of a fixed-lag Kalman smoother for input and state estimation in vibrating structures," *Inverse Problems Sci. Eng.*, vol. 29, no. 9, pp. 1260–1281, 2021.
[11] M. Impraimakis and A. W. Smyth, "An unscented Kalman filter method for real time input-parameter-state estimation," *Mech. Syst. Signal Process.*, vol. 162, 2022, Art. no. 108026.
[12] A. Myklebust and L. Eriksson, "Modeling, observability, and estimation of thermal effects and aging on transmitted torque in a heavy duty truck with a dry clutch," *IEEE/ASME Trans. Mechatron.*, vol. 20, no. 1, pp. 61–72, Jan. 2015.
[13] W. Wei, H. Dourra, and G. G. Zhu, "Transfer case clutch torque estimation using an extended Kalman filter with unknown input," *IEEE/ASME Trans. Mechatron.*, vol. 27, no. 5, pp. 2580–2588, May 2022.
[14] M. Manngård et al., "Estimation of propeller torque in azimuth thrusters," *IFAC-PapersOnLine*, vol. 52, no. 21, pp. 140–145, 2019.
[15] M. Manngård et al., "Torque estimation in marine propulsion systems," *Mech. Syst. Signal Process.*, vol. 172, 2022, Art. no. 108969.
[16] Y. Zhou, X. Wang, and L. Yin, "Estimation of discrete-time linear systems with structural disturbances," in *Proc. 7th Int. Conf. Control Robot. Eng. (ICCRE)*, 2022, pp. 128–132.
[17] T. Ikonen, O. Peltokorpi, and J. Karhunen, "Inverse ice-induced moment determination on the propeller of an ice-going vessel," *Cold Regions Sci. Technol.*, vol. 112, pp. 1–13, 2015.
[18] R. de Waal, A. Bekker, and P. Heyns, "Indirect load case estimation for propeller-ice moments from shaft line torque measurements," *Cold Regions Sci. Technol.*, vol. 151, pp. 237–248, 2018.
[19] B. M. Nickerson and A. Bekker, "Recommendations for regularization in the inverse estimation of ice-induced propeller moments for ice-going vessels," *Cold Regions Sci. Technol.*, vol. 192, 2021, Art. no. 103378.
[20] U. Hakonen, M. Manngrd, S. Laine, and R. Viitala, "Torque reconstruction for maritime powertrains using trend filtering," *IFAC-PapersOnLine*, vol. 58, no. 20, pp. 101–106, 2024.
[21] M. I. Friswell, J. E. T. Penny, S. D. Garvey, and A. W. Lees, *Dynamics of Rotating Machines*, 1st ed. Cambridge, U.K.: Cambridge Univ. Press, Mar. 2010.
[22] G. Genta, *Vibration of Structures and Machines: Practical Aspects*. Berlin, Germany: Springer Science & Business Media, 2012.
[23] S. Laine, U. Hakonen, E. Nieminen, R. Ala-Laurinaho, and R. Viitala, "Opentorsion: Python library for torsional vibration analysis," *SoftwareX*, vol. 29, 2025, Art. no. 102013.
[24] R. J. Hodrick and E. C. Prescott, "Postwar us business cycles: An empirical investigation," *J. Money, Credit, Bank.*, pp. 1–16, 1997.
[25] P. C. Hansen, *The L-Curve and Its Use in the Numerical Treatment of Inverse Problems*, vol. 4. Southampton, U.K.: WIT Press, 2001, pp. 119–142.
[26] S. Haikonen, I. Koene, J. Keski-Rahkonen, and R. Viitala, "Small-scale test bench of maritime thruster for digital twin research," in *Proc. IEEE Int. Instrum. Meas. Technol. Conf. (I2MTC)*, 2022, pp. 1–6.

Urho Hakonen received the B.Sc.(Tech.) and M.Sc.(Tech.) degrees in mechanical engineering from Aalto University, Espoo, Finland, in 2021 and 2023, respectively,

He is currently a Doctoral Researcher with Aalto University. His research interests include torsional vibration, input and state estimation methods, and simulation software.

Mikael Manngård received the M.Sc. (Tech.) degree in process and systems engineering from Åbo Akademi University, Finland, in 2013, where he is currently working toward the Ph.D. degree in process control.

He is currently a Project Manager with the Novia University of Applied Sciences, Finland. His research interests include virtual sensing, system identification, and virtual commissioning techniques.

Sampo Laine received the M.Sc. and D.Sc. degrees from Aalto University, Espoo, Finland, in 2021 and 2025, where he is currently an academic visitor.

His research interests include the dynamics of rotating machinery, torsional vibrations, condition monitoring, and the development of engineering simulation software.

Raine Viitala (Associate Member, IEEE) was born in 1992. He received the M.Sc. and D.Sc. degrees in mechanical engineering from Aalto University, Espoo, Finland, in 2017 and 2018, respectively,

He was appointed Assistant Professor in 2020. He has been a Visiting Researcher with TU Darmstadt, Darmstadt, Germany, and a Visiting Professor with NCSU. He has a strong background in experimental research on large rotors, covering areas, such as vibration analysis, bearing excitations, roundness measurements, and manufacturing for operating conditions. His work has applications in various industrial sectors, including electric motors and generators, turbines, and paper machines. He is actively involved in teaching and mentoring students at all academic levels and serves as the responsible teacher for the Mechatronics minor at Aalto University.